The production and photodissociation of iron–sulfur cluster ions

Zhongde Yu, Nan Zhang, Xiaojun Wu, Zhen Gao,[a] Qihe Zhu, and Fanao Kong
State Key Laboratory of Molecular Reaction Dynamics, Institute of Chemistry, Chinese Academy of Sciences, Beijing 100080, People's Republic of China

(Received 1 March 1993; accepted 20 April 1993)

Iron–sulfur cluster ions $Fe_nS_m^+$ ($n=1$–13, $m=1$–13) were produced by direct laser ablation on a solid sample containing a mixture of iron and sulfur powder. UV photodissociation of the cluster ions was studied with a tandem time-of-flight mass spectrometer. It was found that all the cluster ions with compositions of $m=n$, $m=n-1$, or $m=n+5$ were relatively more abundant, indicating that they were stable. The photodissociation results of the $Fe_nS_m^+$ ions showed that, for parent ions with $n \ll m$, the main channels were sequential losses of neutral S atoms until $n \sim m$, while for parent ions with $n \sim m$, the main product ions had compositions of smaller $m=n$ or $m=n-1$. From these experimental results, it is proposed that the $Fe_nS_n^+$ cluster ions might have structures similar to those of the $Fe_nS_n^*$ cores in iron–sulfur proteins, while the $Fe_nS_m^+$ ($m>n$) cluster ions could be considered to have structures with the $Fe_nS_n^+$ cores surrounded by some peripheral S atoms.

I. INTRODUCTION

The studies of binary clusters composed of transition-metal and nonmetal elements are subjects of great current interest because of their applications in many respects.[1–3] Among them, iron–sulfur clusters are very important in biology.[4–6] Iron–sulfur proteins consist of iron atoms and sulfur-containing ligands called nonheme iron proteins (NHIP). They contain $Fe_nS_n^*$ cluster cores and participate in various redox reactions (electron transfer processes) such as photosynthesis, nitrogen fixation, and mitochondrion respiration in biological bodies. Depending on their different iron–sulfur centers contained, the iron–sulfur proteins take several types—rubredoxin (Rd), plant ferredoxin (Fd), high-potential iron protein (HiPIP), bacterial ferredoxin, *et al.* In addition,a large number of Fe–S protein analogs or complexes have been synthesized inorganically such as in the work of Holm *et al.*,[7–9] including the research on biological nitrogen fixation.[10–12] The study of iron–sulfur clusters has become a frontier in modern bioinorganic chemistry.

In the study of metallic and nonmetallic binary clusters with the methods of laser ablation and mass spectrometry, only a few reports have been published such as $Ta_nC_m^+$ ($n=1$–11, $m=1$–26) (Ref. 1), $Ni_nS_m^+$ ($n=1$–3, $m=1$–2) (Ref. 13), and $Ta_nS_m^+$ ($n=1$–9, $m=1$–30) (Ref. 14), but the study of iron–sulfur clusters with similar methods has not been reported. Unlike the conventional methods dealing with iron–sulfur clusters in the condensed phase, we produced a variety of iron–sulfur cluster ions in the gas phase with the method of laser ablation and studied their UV photodissociation for the first time and also discussed their possible structures.

II. EXPERIMENT

The experiments were performed on a home-built tandem time-of-flight mass spectrometer shown in Fig. 1. The apparatus consists of two stages of mass spectrometers based on Smalley's design.[15] Briefly, the initial acceleration stack in the first-stage mass spectrometer is composed of an array of three stainless steel electrodes with molybdenum grids mounted in the center of chamber 1 and it provides a pulsed two-stage acceleration field. The distance of the first acceleration region is 3 cm and the distance of the second is 1 cm. By adjusting the ratio of the two-stage voltages, the time spread can be minimized and the best set of parameters for high mass resolution can be obtained. In the model of direct laser ablation without carrier gas, a solid sample is located at the side of the first acceleration region in chamber 1 which is maintained at $\sim 10^{-6}$ Torr. The sample is prepared with a mixture of reduced iron powder ($>98.0\%$) and precipitated sulfur powder ($>99.0\%$) in a molar ratio of Fe:S=1:4. The ablation laser (532 nm) is the second harmonic of a pulsed Nd:YAG laser at a repetition rate of 10 Hz. The laser beam is focused with a lens ($f=50$ cm) onto the sample surface, and the laser fluence is $\sim 10^7$–10^8 W/cm^2. The cluster ions produced travel freely in the direction opposite to that of laser beam, then pass through a hole with a diameter of $\phi=7$ mm located in front of the sample into the first acceleration region. The time delay between the laser fire and the pulsed acceleration field is properly selected in order to collect those cluster ions which have small velocity spread. The pulsed two-stage acceleration field is provided by a home-built high-voltage pulse generator (1200 V maximum, adjustable pulse duration). The high voltage pulse generated by it has excellent pulse shape (with rise and fall times of 0.2 μs) and is nicely reproducible. The first flight tube is at ground potential. Two sets of deflection plates are mounted right after the last acceleration plate which is also kept at ground potential. Then two sets of Einzel lenses are followed to

[a]Author to whom correspondence should be addressed.

 0021-9606/93/99(3)/1765/6/$6.00

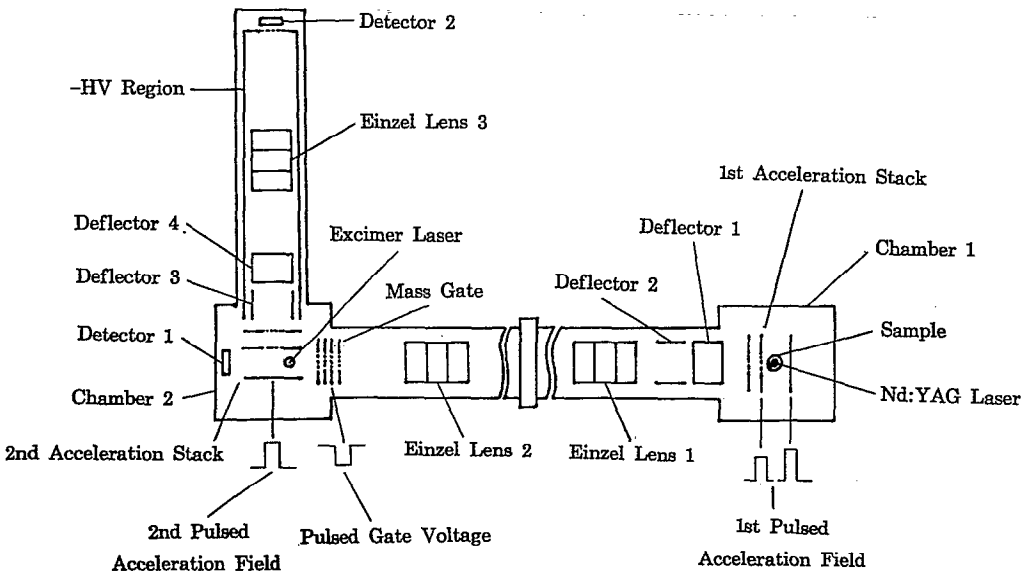

FIG. 1. A schematic diagram of the tandem time-of-flight mass spectrometer (TOFMS).

reduce the radial space distribution of the cluster ions. The first Einzel lens follows immediately the deflection plates, and the second one sits approximately 1.5 m downstream. The flight tube of 3.4 m length gives a mass resolution of ~300. At the end of the first flight tube is another array of four stainless steel electrodes separated 6 mm from each other. This stack combines the function of mass selection and deceleration. The width of the mass gate (i.e., the width of pulsed gate voltage) is typically 0.5–3 μs with rise and fall times of 20–30 ns, and all the unneeded ions can be cut off effectively. The selected cluster ions are decelerated to <100 eV and travel into an initially field-free region in chamber 2. A dual microchannel plate detector is fixed at the end of the region either to monitor the mass distribution of the cluster ions produced when the mass gate is not active, or to monitor the mass selection when the mass gate is active. In the experiment of photodissociation, the decelerated cluster ion packet in chamber 2 is crossed by an excimer laser beam (Lumonics, KrF, 248 nm) and the photodissociation process takes place. As the parent ions and all the photoproducts pass through the gridded aperture in the center of the second acceleration assembly, these ions are accelerated into the second flight tube which is perpendicular to the first one. The acceleration voltage is again adjustable to optimize the mass resolution. In the second acceleration stage, the voltage drops from the deceleration potential to a high negative voltage (<-2500 V) at which the entire second flight tube is floated. Two deflectors perpendicular to each other and an Einzel lens, which have the same functions as those in the first-stage time-of-flight mass spectrometer, direct the product ions passing through a field-free region of 1.5 m and reaching another dual microchannel plate detector fixed at the end of the region. The signals from the detectors are preamplified then recorded with a transient recorder (10 or 100 MHz), and finally accumulated up to several thousand times and stored in an IBM PC.

III. RESULTS AND DISCUSSION

A. Formation of iron–sulfur cluster ions $Fe_nS_m^+$

It has been known that the distribution of cluster size depends greatly on the growth conditions in cluster source.[16] In the experiment of cluster formation by direct laser ablation, the laser fluence, the laser spot on sample surface, and the depth of crater in sample all change the cluster distribution.

A typical first-stage TOF mass spectrum of iron–sulfur cluster ions $Fe_nS_m^+$ ($m=1$–13, $n=1$–13) is shown in Fig. 2. This spectrum was obtained by averaging over 1000 laser shots with laser fluence of $\sim 10^7$ W/cm^2 and laser spot diameter of ~0.1 mm on the sample surface. Although there are several other factors which affect the intensity of the mass peak, such as the formation mechanism and the ionization efficiency of the cluster ions, and the sensitivity of detector,[16] it can be assumed under our experimental

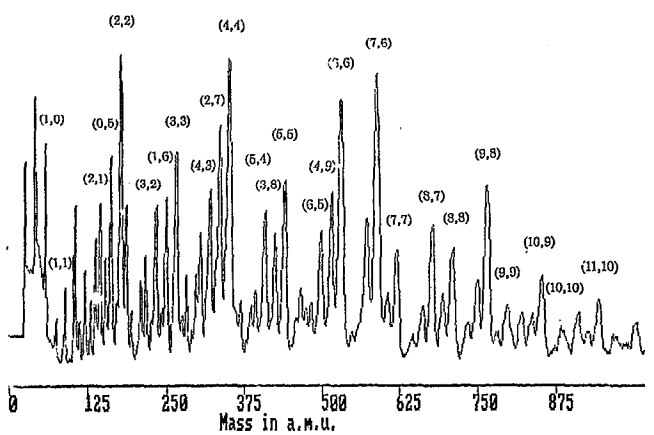

FIG. 2. The mass spectrum of $Fe_nS_m^+$ cluster ions obtained in the first-stage TOFMS.

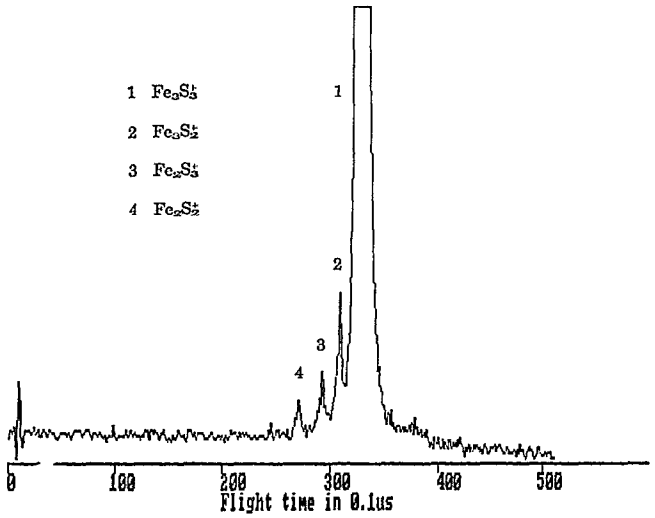

FIG. 3. The mass spectrum of the $Fe_3S_3^+$ parent ion and its product ions obtained in the second-stage TOFMS.

conditions that the intensities of the mass peaks represent basically the relative stability of the cluster ions. Comparing the intensities of the mass peaks with the same n, but different m in the spectrum, it is clear that the most intense peaks have nearly equal numbers of Fe and S atoms. For $n=2$–6, the $m=n$ peaks are the most intense and the $m=n-1$ ones are second, while for $n=7$–11, the $m=n-1$ peaks are the most intense and the $m=n$ ones are second. Furthermore, comparing the most intense peaks in the spectrum, for $n=2$–6, the $m=n$ ones with even number n are more intense, while for $n=7$–10, the $m=n-1$ ones with odd number n are more intense.

It has also been found that there exist another group of cluster ions with compositions of $m=n+5$ which has local maximum intensity. In addition, several pure sulfur cluster ions S_m^+ ($m=4$–7) are observed with the most intense one of S_5^+, which is similar to the result of sulfur cluster ions produced from pure sulfur sample,[17] so it might be shown that $Fe_nS_n^+$ cluster ions are easily combined with S_5 to form $Fe_nS_{n+5}^+$. As for the pure iron cluster ions Fe_n^+, the $n=1$ peak is the most intense. It should be noted that the atomic weights of iron and sulfur have a common factor of 8, i.e., the weight of seven sulfur atoms is equal to that of four iron atoms. This fact leads to an uncertainty for the assignment of cluster composition, but such a problem can be partly solved by the photodissociation results of the cluster ions.

B. UV photodissociation of iron–sulfur cluster ions

The $Fe_nS_m^+$ cluster ions were selected individually by the mass gate in the tandem TOF mass spectrometer and then irradiated by 248 nm UV laser. The dependence of the daughter ions upon laser fluence was obtained by observing the change of mass spectrum. In the laser fluence more than 1 mJ/cm^2, it was shown that the photofragmentation resulted from the multiphoton process.

Figure 3 shows an example of the photodissociation with laser fluence of ~ 5 mJ/cm^2. The parent ion is $Fe_3S_3^+$, and the product ions are $Fe_3S_2^+$, $Fe_2S_3^+$, and $Fe_2S_2^+$. For FeS_m^+ ($m=2$–8), $Fe_2S_m^+$ ($m=0$–8), and $Fe_3S_m^+$ ($m=2$–9), the photodissociation channel and the corresponding fractional parent ion loss are listed in Table I. In general, when the number of S atoms is much larger than that of Fe atoms in parent cluster ions ($m>n$), the main dissociation patterns are losses of S, S_2, or S_4. (The exceptions are $Fe_3S_8^+$ and $Fe_3S_9^+$, which have neutral FeS_2 loss.) Table II summarizes the photodissociation channels and the corresponding branching ratios of the parent cluster ions with $m=n$ and $m=n-1$. The results indicate that, for $n\sim m$, there exist several photodissociation fashions such as the elimination of either the Fe atom, S atom, or both atoms. In short, all the iron–sulfur cluster ions with the most and second intense peaks, after UV photodissociation, give the products with compositions of smaller $m=n$ or $m=n-1$. This fact confirms that the $Fe_nS_n^+$ and $Fe_nS_{n-1}^+$ cluster ions have very stable structures.

TABLE I. Photodissociation of iron–sulfur cluster ions $Fe_nS_m^+$ ($n=1$–3, $m=0$–9).

Parent ion	Neutral loss							Fractional parent ion loss
	S	S_2	S_3	S_4	Fe	FeS	FeS_2	
FeS_2^+	1.4							1.4
FeS_3^+	2.4							2.4
FeS_4^+	1.3	2.6						3.9
FeS_5^+		3.4						3.4
FeS_6^+	3.3	2.9						6.2
FeS_7^+		6.0	2.5	10.0				18.5
FeS_8^+		5.0		27.0				32.0
Fe_2^+					0.7			0.7
Fe_2S^+	3.8				3.0	1.6		8.4
$Fe_2S_2^+$	3.6							3.6
$Fe_2S_3^+$	6.1	7.7						13.8
$Fe_2S_4^+$		5.3						5.3
$Fe_2S_5^+$		3.8						3.8
$Fe_2S_6^+$				9.1				9.1
$Fe_2S_7^+$				9.1				9.1
$Fe_2S_8^+$		2.1		18.5				20.6
$Fe_3S_2^+$					4.8			4.8
$Fe_3S_3^+$	2.5				1.6	1.1		5.2
$Fe_3S_4^+$	3.3	3.8						7.1
$Fe_3S_5^+$		9.4						9.4
$Fe_3S_6^+$		8.6		12.2				20.8
$Fe_3S_7^+$		4.7		7.1				11.8
$Fe_3S_8^+$		14.0					7.5	21.5
$Fe_3S_9^+$		4.2					8.3	12.5

C. The possible structures of some $Fe_nS_m^+$ cluster ions

The study of the structures of iron–sulfur clusters has a long history. From x-ray crystallography, it has been confirmed that there exist iron–sulfur clusters in iron–sulfur proteins such as 1Fe–4S {[Fe(S–Cys)$_4$], S-Cys =cysteinyl residues} in rubredoxin,[18] 2Fe–2S* {[$Fe_2S_2^*$(S-Cys)$_4$], S* is labile sulfur} in plant ferredoxin,[19] 4Fe–4S* {[$Fe_4S_4^*$(S-Cys)$_4$]} in high-potential iron protein,[20] 8Fe–8S* (two 4Fe–4S*),[21] and 3Fe–3S* redox cen-

TABLE II. Photodissociation of iron–sulfur cluster ions $Fe_nS_m^+$ (n=2–8, m=n, n–1).

Parent ion	Photodissociation channel	Branching ratio (%)
$Fe_2S^+ \rightarrow$	$Fe_2^+ + S$	45
	$FeS^+ + Fe$	36
	$Fe^+ + FeS$	19
$Fe_2S_2^+ \rightarrow$	$Fe_2S^+ + S$	100
$Fe_3S_2^+ \rightarrow$	$Fe_2S_2^+ + Fe$	100
$Fe_3S_3^+ \rightarrow$	$Fe_3S_2^+ + S$	48
	$Fe_2S_3^+ + Fe$	31
	$Fe_2S_2^+ + FeS$	21
$Fe_4S_3^+ \rightarrow$	$Fe_3S_3^+ + Fe$	77
	$Fe_3S_2^+ + FeS$	23
$Fe_4S_4^+ \rightarrow$	$Fe_4S_3^+ + S$	71
	$Fe_3S_3^+ + FeS$	29
$Fe_5S_4^+ \rightarrow$	$Fe_4S_4^+ + Fe$	28
	$Fe_4S_2^+ + FeS_2$	72
$Fe_5S_5^+ \rightarrow$	$Fe_4S_4^+ + FeS$	100
$Fe_6S_5^+ \rightarrow$	$Fe_5S_5^+ + Fe$	38
	$Fe_5S_3^+ + FeS_2$	51
	$Fe_4S_3^+ + Fe_2S_2$	11
$Fe_6S_6^+ \rightarrow$	$Fe_6S_4^+ + S_2$	58
	$Fe_5S_5^+ + FeS$	5
	$Fe_5S_4^+ + FeS_2$	11
	$Fe_4S_4^+ + Fe_2S_2$	26
$Fe_7S_6^+ \rightarrow$	$Fe_6S_6^+ + Fe$	68
	$Fe_6S_4^+ + FeS_2$	32
$Fe_7S_7^+ \rightarrow$	$Fe_7S_6^+ + S$	38
	$Fe_6S_7^+ + Fe$	31
	$Fe_6S_6^+ + FeS$	31
$Fe_8S_7^+ \rightarrow$	$Fe_7S_7^+ + Fe$	45
	$Fe_7S_6^+ + FeS$	55
$Fe_8S_8^+ \rightarrow$	$Fe_8S_6^+ + S_2$	23
	$Fe_7S_6^+ + FeS_2$	77

ter in bacterial ferredoxin.[22] In addition, a large number of iron–sulfur protein analogs with a mononuclear center of $[Fe(S_2\text{-}o\text{-xyl})_2]^{2-,1-}$ (S_2-o-xyl=o-xylyl-α, α'-dithiolate),[23] the binuclear center of $[Fe_2S_2^*(SR)_4]^{2-}$ (R=alkyl,aryl),[24] and tetranuclear center of $[Fe_4S_4^*(SR)_4]^{2-}$,[25] as well as several other iron–sulfur complexes with less direct biological relevance such as $[Fe_6S_6^*(L)_6]^{3-}$ (L=Cl, Br, I, RS, and RO),[26] $Fe_7S_6^*(PEt_3)_4Cl_3$ (Et=ethyl),[27] $[Fe_3(S^*Ph)_3Cl_6]^{3-}$ (Ph=phenyl),[28] and $[Fe_4S_5^*Cp_4]^{2+}$ (Cp=π-cyclopentadienyl)[29] have been synthesized. The structures of the iron–sulfur cores in these analogs and complexes have also been determined by the x-ray diffraction method, and the core structures of the 2Fe and 4Fe analogs are entirely consistent with those of the active sites in the corresponding 2Fe and 4Fe proteins.

As for the structures of iron–sulfur cluster ions produced by laser ablation, some features can be obtained by analyzing the experimental results, although it is impossible to clear their structures only from mass spectrum and photodissociation. It was presented in our experiment that all the $Fe_nS_n^+$ (n=2–6) and $Fe_nS_{n-1}^+$ (n=7–11) cluster ions were more stable and the main photodissociation channels of $Fe_nS_m^+$ ($m\sim n$) were the formation of $Fe_nS_n^+$ or $Fe_nS_{n-1}^+$ with smaller n. It has been known that the compositions of the $Fe_nS_n^+$ cluster ions are as same as those of the $Fe_nS_n^*$ cores in proteins, so it is reasonable to compare the $Fe_nS_n^+$ cluster ions with the iron–sulfur cluster cores in proteins and their synthetic analogs or complexes, and to propose structural models for the iron–sulfur cluster ions produced by laser ablation. In general, the iron–sulfur cluster ions $Fe_nS_n^+$ are stable cores which can be ligated by sulfur atoms to form $Fe_nS_m^+$ ($m>n$). The structures of some typical $Fe_nS_n^+$ cluster ions are discussed in detail as follows:

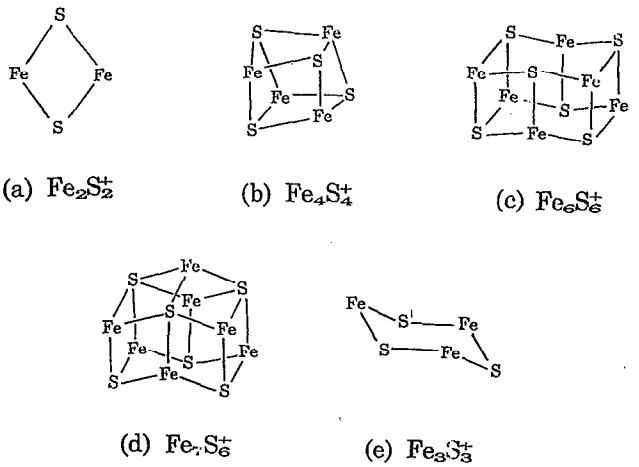

FIG. 4. Possible structures of some typical $Fe_nS_n^+$ cluster ions.

1. $Fe_2S_2^+$

On the results of experiment, it is proper that the $Fe_2S_2^+$ ion might have a structure similar to that of the rhombic $Fe_2S_2^*$ core in protein shown in Fig. 4(a).[24] This structure is a planar rhombic unit in which the two Fe atoms are linked through two sulfur bridges and a weak Fe–Fe metallic bond without interaction between sulfur atoms. This is a stable structure, and under UV laser irradiation, it is easier for the $Fe_2S_2^+$ ion to lose one S atom than to lose one Fe atom, and the product Fe_2S^+ ion might be expected to contain a single bridging sulfur atom $(Fe\text{–}S\text{–}Fe)^+$.

2. $Fe_4S_4^+$

This cluster ion is stable presented in the first-stage mass spectrum. The main photodissociation channel is neutral S atom loss to yield $Fe_4S_3^+$, while the secondary channel is neutral FeS loss to form $Fe_3S_3^+$. The results make us believe that the $Fe_4S_4^+$ cluster ion has a distorted cubane-like configuration such as that of the $Fe_4S_4^*$ core in 4Fe protein and its synthetic analog shown in Fig. 4(b).[25] The $Fe_4S_4^*$ core of $[Fe_4S_4^*(SR)_4]^{2-}$ analog, e.g., is a distorted cube with Fe and S* atoms at alternate vertices and exhibits perceptible distortions from cubic (T_d) symmetry to the point group D_{2d}–$\bar{4}2m$.[25] Each face of the $Fe_4S_4^*$ polyhedron is a rhomb and is distinctly nonplanar. This structure is actually the combination of two $Fe_2S_2^*$ rhombic units. It might be expected, under the irradiation of UV

laser, to lose one sulfur atom at a vertex at first and then to lose one iron atom. The final product ion $Fe_3S_3^+$ might have a distorted six-membered ring conformation such as the $Fe_3S_3^*$ core in 3Fe protein or its synthetic complex.[22,28]

3. $Fe_6S_6^+$ and $Fe_7S_6^+$

These two cluster ions are also very intense in the first-stage mass spectrum. The $Fe_6S_6^+$ ion might possess a distorted hexagonal prismane configuration with six Fe and six S atoms occupying the alternating vertices just as the $Fe_6S_6^*$ core in the 6Fe complex shown in Fig. 4(c).[26] The $Fe_6S_6^*$ core can be analyzed in terms of two identical cyclohexane-chair $Fe_3S_3^*$ units eclipsed relative to each other and oriented in a way that the S* atoms from one unit serve as ligands for the Fe atoms in the other. The $Fe_6S_6^*$ core can be described also in terms of three $Fe_2S_2^*$ planar rhombic units fused so as to yield the hexagonal prismatic arrangement. With this structure, it might be easier, under irradiation of UV laser, to lose S atoms than to lose Fe atoms, which is consistent with the photodissociation result, i.e., the main channel is losing two S atoms. The secondary channel is neutral Fe_2S_2 loss to the remaining $Fe_4S_4^+$ ion, which is similar to the conclusion[26] that the $(Fe_6S_6)^{3+}$ core in the synthetic 6Fe complex appears to be a metastable entity and is easily transformed, upon heating, to the thermodynamically more stable $(Fe_4S_4)^{2+}$ core. For the $Fe_7S_6^+$ ion, its main photodissociation channel is neutral Fe atom loss. If the $Fe_7S_6^+$ ion has the monocapped prismatic configuration as the $Fe_7S_6^*$ core in the 7Fe complex shown in Fig. 4(d),[27] it might lose the Fe atom at the vertex of the "cap" under irradiation of the UV laser, in agreement with our experimental result.

4. $Fe_3S_3^+$ and $Fe_5S_5^+$

These two cluster ions have weaker intensities than those of $Fe_2S_2^+$, $Fe_4S_4^+$, and $Fe_6S_6^+$, revealing the relative instability of the iron–sulfur cluster ions containing odd numbers of Fe atoms and S atoms. The main photodissociation channel of $Fe_3S_3^+$ is neutral S atom loss, while the secondary channel is neutral loss of Fe, or FeS. The structure of the $Fe_3S_3^+$ ion is shown in Fig. 4(e) being a distorted six-membered ring such as the $Fe_3S_3^*$ core in 3Fe protein[22] or the synthetic complex.[28] As for the $Fe_5S_5^+$ cluster ion, it must be mentioned that, as we know, the 5Fe–5S* cluster has not been discovered yet in any protein, and its analog or complex has not been synthesized either. However, our experimental result indicates that the $Fe_5S_5^+$ cluster ion does exist although it is relatively unstable. The $Fe_5S_5^+$ cluster ion was photodissociated with the main channel of neutral FeS loss to yield the $Fe_4S_4^+$ ion. On the photodissociation result, it can be imagined that the $Fe_5S_5^+$ cluster ion might have such a structure as a $Fe_4S_4^+$ cubic unit with FeS added or similar to the cage-like structure of the $Fe_4S_5^*$ complex.[29] It can be expected that the 5Fe–5S* iron–sulfur cluster might be discovered in proteins and its analog or complexes containing the $Fe_5S_5^*$ cluster core might be synthesized in the future.

IV. CONCLUSION

Iron–sulfur cluster ions $Fe_nS_m^+$ (n, $m=1$–13) were obtained by direct laser ablation from a solid sample, and UV photodissociation of these cluster ions was studied with a tandem time-of-flight mass spectrometer. It was found that the iron–sulfur cluster ions with compositions of $m=n$, $m=n-1$, or $m=n+5$ had large abundances, while the dissociation channels of $Fe_nS_m^+$ were neutral losses of S, S_2, S_4, Fe, FeS, or FeS_2, etc., and the main product ions had compositions of smaller $m=n$ or $m=n-1$. From the experimental results, it can be inferred that the $Fe_nS_n^+$ cluster ions might have structures similar to those of the Fe_nS_n cluster cores in iron–sulfur proteins, while the $Fe_nS_m^+$ ($m>n$) cluster ions might have $Fe_nS_n^+$ cores surrounded by more peripheral sulfur atoms.

ACKNOWLEDGMENT

This work was supported by the National Natural Science Foundation of China.

[1] S. W. McElvany and C. J. Cassady, J. Phys. Chem. **94**, 2057 (1990).
[2] E. I. Stiefel, T. R. Halbert, C. L. Coyle, L. Wei, W.-H. Pan, T. C. Ho, R. R. Chianelli, and M. Daage, Polyhedron **8**, 1625 (1989).
[3] S. A. Sunshine, D. A. Keszler, and J. A. Ibers, Acc. Chem. Res. **20**, 395 (1987).
[4] B. Kerbs and G. Henkel, Angew. Chem. Int. Ed. Engl. **30**, 769 (1991).
[5] *Iron–Sulfur Proteins*, edited by W. Lovenberg (Academic, New York, 1973 and 1977), Vols. 1–3.
[6] P. F. Shen, H. L. Chen, and B. Y. Yu, *Modern Inorganic Chemistry* (Shanghai Science and Technology, Shanghai, 1985).
[7] R. H. Holm, Acc. Chem. Res. **10**, 427 (1977).
[8] R. H. Holm, Chem. Soc. Rev. **10**, 455 (1981).
[9] J. M. Bery and R. H. Holm, in *Iron Sulfur Proteins*, edited by T. G. Spiro (Wiley, New York, 1982).
[10] *Nitrogen Fixation—the Chemical–Biochemical–Genetic Interface*, edited by A. Müller and W. Newton (Plenum, New York, 1983).
[11] S. P. Cramer, K. O. Hodgson, W. O. Gillum, and L. E. Mortenson, J. Am. Chem. Soc. **100**, 3398 (1987).
[12] J. X. Lu and B. T. Zhuang, Jiegou Huaxue **8**, 233 (1989).
[13] I. H. Musselman, R. W. Linton, and D. S. Simons, Anal. Chem. **60**, 110 (1988).
[14] N. Zhang, Z. D. Yu, X. J. Wu, Z. Gao, Q. H. Zhu, and F. A. Kong, J. Chem. Soc. Faraday Trans. (in press).
[15] S. C. O'Brien, J. R. Heath, R. F. Curl, and R. E. Smalley, J. Chem. Phys. **88**, 220 (1988).
[16] E. A. Rohlfing, J. Chem. Phys. **93**, 7851 (1990).
[17] N. Zhang, Z. Gao, F. A. Kong, and Q. H. Zhu, Prog. Natural Sci. (China) **3**, 170 (1993).
[18] J. R. Herriott, L. C. Sieker, and L. H. Jenson, J. Mol. Biol. **50**, 391 (1970).
[19] T. Tsukihara, K. Fukuyama, H. Tahara, Y. Katsube, Y. Matsuura, N. Tanaka, M. Kakudo, K. Wada, and H. Matsubara, J. Biochem. (Tokyo) **84**, 1645 (1978).
[20] C. W. Carter, Jr., S. T. Freer, N. H. Xuong, R. A. Alden, and J. Kraut, Cold Spring Harbor Symp. Quant. Biol. **36**, 381 (1971).
[21] L. C. Sieker, E. Adman, and L. H. Jenson, Nature (London) **235**, 40 (1972).
[22] D. Ghosh, S. O'Donnell, W. Furry, Jr., A. H. Robbins, and C. D. Stout, J. Mol. Biol. **158**, 73 (1982).
[23] R. W. Lane, J. A. Ibers, R. B. Frankel, and R. H. Holm, Proc. Natl. Acad. Sci. U. S. A. **72**, 2868 (1975).
[24] J. J. Mayerle, S. E. Denmark, B. V. DePamphilis, J. A. Ibers, and R. H. Holm, J. Am. Chem. Soc. **97**, 1032 (1975).

[25] B. A. Averill, T. Herskovitz, R. H. Holm, and J. A. Ibers, J. Am. Chem. Soc. **95**, 3523 (1973).
[26] M. G. Kanatzidis, W. R. Hagen, W. R. Dunham, R. K. Lester, and D. J. Coucouvanis, J. Am. Chem. Soc. **107**, 953 (1985).
[27] I. Noda, B. S. Snyder, and R. H. Holm, Inorg. Chem. **25**, 3851 (1986).
[28] K. S. Hagen and R. H. Holm, J. Am. Chem. Soc. **104**, 5496 (1982).
[29] N. Dupré, P. Auric, H. M. J. Hendriks, and J. Jordanov, Inorg. Chem. **25**, 1391 (1986).